Discovery of novel tricyclic pyrido[3',2':4,5]thieno[3,2-d]pyrimidin-4-amine derivatives as VEGFR-2 inhibitors

ARTICLE *in* BIOORGANIC CHEMISTRY · APRIL 2015

Impact Factor: 2.15 · DOI: 10.1016/j.bioorg.2015.03.004

Bioorganic Chemistry 60 (2015) 1–12

Contents lists available at ScienceDirect

Bioorganic Chemistry

journal homepage: www.elsevier.com/locate/bioorg

Discovery of novel tricyclic pyrido[3′,2′:4,5]thieno[3,2-*d*]pyrimidin-4-amine derivatives as VEGFR-2 inhibitors

Yasmine M. Abdel Aziz [a,*], Mohamed M. Said [a], Hosam A. El Shihawy [a], Khaled A.M. Abouzid [b]

[a] Pharmaceutical Organic Chemistry Department, Faculty of Pharmacy, Suez Canal University, Ismailia, Egypt
[b] Pharmaceutical Chemistry Department, Faculty of Pharmacy, Ain Shams University, Cairo, Egypt

ARTICLE INFO

Article history:
Received 22 February 2015
Available online 4 April 2015

Keywords:
Pyridothienopyrimidine
Kinase
VEGFR-2
Inhibitors
Docking studies

ABSTRACT

In an effort to develop ATP-competitive VEGFR-2 selective inhibitors, a novel series of tricyclic pyrido[3′,2′:4,5]thieno[3,2-*d*]pyrimidin-4-amine derivatives were designed and synthesized. These compounds were characterized by IR, ^{1}H NMR, ^{13}C NMR, elemental and mass spectral analyses. Docking studies have given a partial insight into the molecular determinants of the activity of this novel series in VEGFR-2 kinase active site. Moreover, these compounds were assessed at 10 μM for their selective inhibitory activities over a panel of 6 human kinases, namely VEGFR-1/Flt-1, VEGFR-2/KDR, EGFR, CDK5/p25, GSK3α and GSK3β. Compound *N*-(4,6-dimethylthieno[2,3-*b*]pyridine)-7,9-dimethylpyrido[3′,2′:4,5]thieno[3,2-*d*]pyrimidin-4-amine **(9d)** exhibited the most potent and selective inhibitory activity against VEGFR-2/KDR over the six human kinases, with an IC_{50} value 2.6 μM. The identification of this hit candidate could aid the design of new tricyclic-based VEGFR-2 kinase modulators.

1. Introduction

In recent years, the field of cancer therapy has witnessed the emergence of the kinase family as one of the most intensively pursued target classes [1]. The role of kinases in tumourigenesis is evident in their ability to transform normal cells into neoplastic phenotypes when they are produced in abnormal high levels [2]. Protein kinases can be broadly classified with respect to substrate specificity into serine/threonine and tyrosine kinases. The former includes cyclin dependant kinase (CDK5) and glycogen synthase kinases (GSK3α and GSK3β). The latter comprises the epidermal growth factor receptor (EGFR) and the vascular endothelial growth factor receptors (VEGFR-1/Flt-1, VEGFR-2/KDR and VEGFR-3) [3–5]. Generally, protein kinases possess a highly conserved domain "an ATP binding site", which is important for the transfer of the γ-phosphate of ATP to protein substrates. Therefore, this induces a conformational change from an inactive to an active form of the protein. Whereas the ATP binding site is very similar in all kinases, each member of the kinase family has characteristic hydrophobic regions in the close vicinity of the ATP binding site, allowing for the design of selective inhibitors [6].

Numerous multikinase inhibitors MKIs have been recently approved for treating cancer. However, gaining a selectivity for a specific kinase is crucial to avoid the off-target activity of MKIs as it might translate into undesirable side effects [7]. Quinazoline and other scaffolds are common in the design of ATP-competitive kinase inhibitors [8]. However, emerging resistance of tumour cells necessitates the continuous search for novel scaffolds that could offer further opportunities to develop more selective kinase inhibitors [9,10].

VEGFR-2 has been identified as the principal regulator of angiogenesis, the process of generating new blood vessels that are important in tumour growth and metastasis [7,11–15]. The development of selective VEGFR-2 inhibitors is of interest as they might provide promising anticancer agents with minimal toxicity [1]. Therefore, much effort has been focused on identifying novel VEGFR-2 selective inhibitors [7,16–18]. It is worth noting that efforts exerted to identify selective inhibitors of a particular kinase often begin with the screening of the archived inhibitors that were developed in previous studies. Hence, the analogue synthesis and the isosteric replacement approaches are generally initiated with a lead scaffold that was primarily identified as a promising inhibitor of a particular kinase [6]. In the light of this, a number of literatures appeared recently on the basis of bioisosteric replacement of the benzene ring of quinazoline-based kinase inhibitors with a thiophene ring [16,19–21]. Munchhof and co-workers reported the design and structure activity relationship (SAR) of a novel

* Corresponding author at: School of Pharmacy, Suez Canal University, New Campus, Ismailia 41522, Egypt. Fax: +20 64 3230741.
E-mail address: mohamad_yasmine@yahoo.com (Y.M. Abdel Aziz).

http://dx.doi.org/10.1016/j.bioorg.2015.03.004
0045-2068/

series of thienopyrimidine derivatives bearing a bicyclic aromatic amine at position 4 (Fig. 1) [16]. The study demonstrated two main modifications. The first modification was based on the addition of a methyl group to the indole ring. Meanwhile the second modification was stood on the replacement of the pyrimidine ring with a pyridine moiety. These modifications have inverted the selectivity of the target compounds between EGFR and VEGFR-2 [16]. However, even with these variations, the most of the synthesized compounds are still equipotent against both targets. In an attempt to address this issue, Gangjee and co-workers designed a novel series of tricyclic pyrimido[4,5-*b*]indole as ATP-competitive inhibitors targeting VEGFR-2 [7]. 5-Chloro-*N*-phenyl-9*H*-pyrimido[4,5-*b*]indole-2,4-diamine has displayed the most selective inhibitory activity against VEGFR-2 over the other closely related kinases (Fig. 1). Despite being suitable drug lead, this compound has possessed only a weak inhibitory activity against VEGFR-2 with IC_{50} value 138 μM [7].

To meet the requirements of enhancing the library of the ATP-competitive VEGFR-2 inhibitors, we herein describe the synthesis of a novel tricyclic pyrido[3′,2′:4,5]thieno[3,2-*d*]pyrimidin-4-amine scaffold. Our target compounds were conceived as a tricyclic congener of 4-aminoquinazoline pharmacophore that is the core in various clinically approved ATP-competitive VEGFR-2 inhibitors such as vandetanib and cediranib (Fig. 1). The design of this novel scaffold was based on three main strategies in order to fit optimally to the VEGFR-2 binding site (Fig. 1). The first strategy was performed by the replacement of the benzenoid moiety of the quinazoline ring with the thiophene ring bioisostere [21]. The second strategy was the fusion of a third ring containing one basic nitrogen such as pyridine to improve the solubilization and to confer a more favourable pharmacokinetic profile [22]. The third strategy, regarding our approach, was the incorporation of novel bicyclic heteroaryl amines at position 4 that could recognize the characteristic hydrophobic regions of VEGFR-2.

2. Experimental

2.1. Chemistry

The structures of all tested compounds were confirmed by ^{1}H NMR, ^{13}C NMR and mass spectrometry (EI-MS). The purities of the tested compounds were determined by elemental analysis. The commercial chemicals and solvents were reagent grade and used without further purification. ^{1}H and ^{13}C NMR Spectra were measured in DMSO-d_6 on a Varian Mercury VX-300 NMR spectrometer or Jeol LA (400 MHz for ^{1}H NMR, 100 MHz for ^{13}C NMR). Chemical shifts were reported in parts per million (ppm)

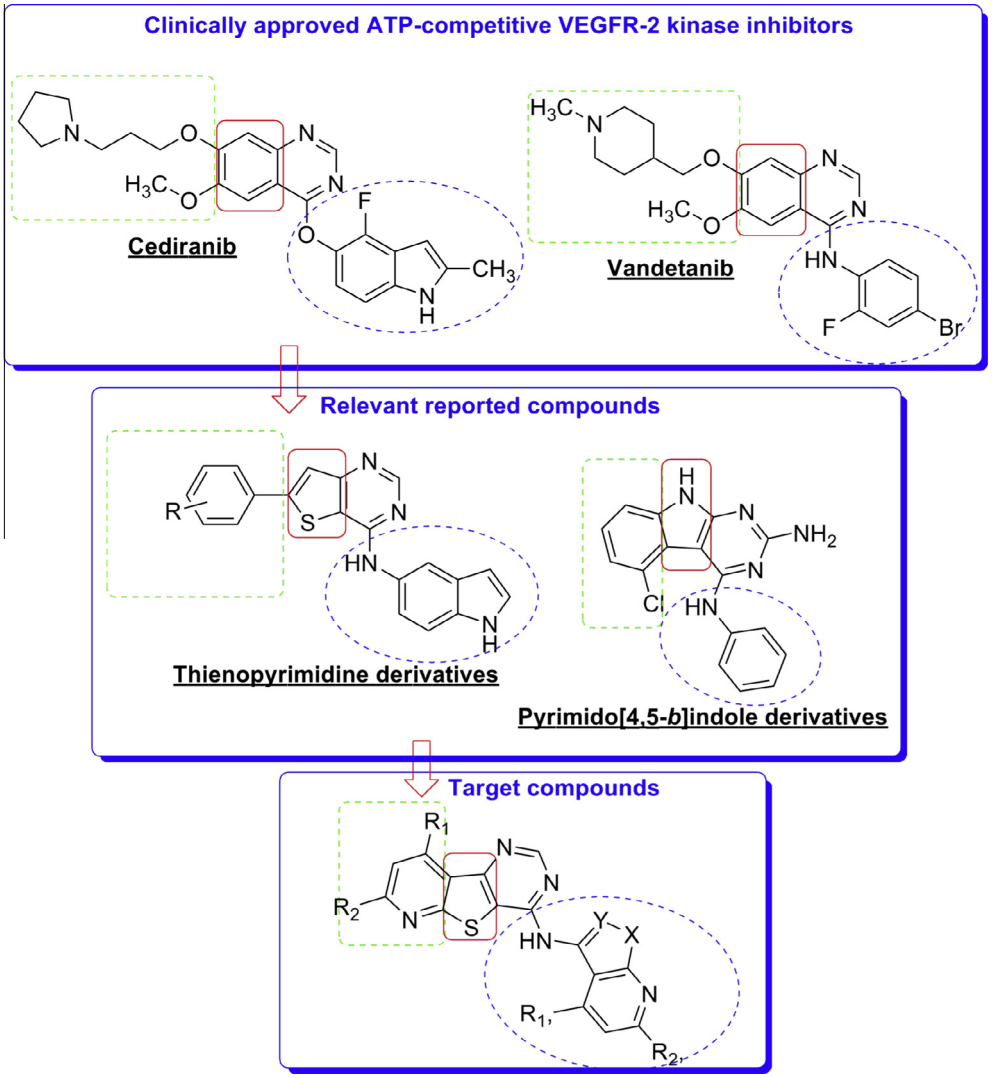

Fig. 1. Design of target compounds as ATP-competitive VEGFR-2 selective inhibitors.

using tetramethylsilane (TMS) as an internal standard. Electron impact mass spectra were recorded on Shimadzu GCMS-QP 5050A gas chromatograph mass spectrometer (70 eV). Elemental analysis was performed at the Microanalytical Center of Cairo University, Egypt. IR spectra were recorded on a Shimadzu FT-IR 8101 PC IR spectrophotometer (KBr pellets). Values were represented in cm^{-1}. The synthetic procedures for the target compounds are illustrated in Schemes 1 and 2.

*2.1.1. 3-Aminothieno[2,3-b]pyridine-2-ethyl carboxylate (**2a**)*

A mixture of 2-chloro-3-cyanopyridine **(1a)** (3.17 g, 20 mmol), ethyl 2-mercaptoacetate (3.62 g, 30 mmol), Na_2CO_3 (2.62 g, 20 mmol) and dry ethanol (12 mL) was refluxed for 4.5 h in darkness under dry conditions. The reaction mixture was allowed to reach the ambient temperature and added to water (150 mL). The resultant precipitate was stirred for 45 min and filtered off. The filter cake was washed with water (2 × 25 mL), dried in vacuum and recrystallised from ethanol to produce the title compound as yellow crystals (3.01 g, 13.5 mmol, 95.1%); mp 137–138 °C [23].

*2.1.2. 3-Amino-4,6-dimethylthieno[2,3-b]pyridine-2-ethyl carboxylate (**2b**)*

Ethyl 2-mercaptoacetate (24.48 g, 200 mmol) and 2-chloro-3-cyano-4,6-dimethylpyridine **(1b)** (33.86 g, 200 mmol) were added to a solution of sodium ethoxide under nitrogen atmosphere, prepared from finely divided sodium metal (4.69 g, 200 mmol) and dry ethanol (468 mL). The mixture was refluxed for 6 h in darkness under dry conditions. It was then allowed to reach the ambient temperature and the precipitate was collected by filtration, triturated with cold water (50 mL) and filtered. The resulting solid was dried in vacuum and recrystallised from ethanol to give light yellow crystals (29.45 g, 117.8 mmol, 87%); mp 157–158.5 °C [24].

*2.1.3. General procedures adapted for the synthesis of 3-formylaminothieno[2,3-b]pyridine derivatives (**3a**, **b**)*

A mixture of starting compound **(2a** or **b)** (10 mmol) and aqueous formic acid (10 mmol, 85% v/v) in toluene (20 mL) were heated under reflux using a Dean–Stark trap for 6–9 h until TLC showed no trace of starting material. The reaction mixture was evaporated under reduced pressure. The purity of the resulting solid was satisfactory for further use [25].

*2.1.4. 3-Formylaminothieno[2,3-b]pyridine-2-ethyl carboxylate (**3a**)*

Bright yellow powder; yield (1.3 g, 5.2 mmol, 59%); mp 243–244 °C [26].

*2.1.5. 3-Formylamino-4,6-dimethylthieno[2,3-b]pyridine-2-ethyl carboxylate (**3b**)*

Pale yellow powder; yield (1.5 g, 5.4 mmol, 60%); mp 267–268.5 °C [26].

*2.1.6. General procedures adapted for the synthesis of pyrido[3′,2′:4,5]thieno[3,2-d]pyrimidin-4-one derivatives (**4a**, **b**)*

Ammonium formate (5.10 g, 80 mmol) and formamide (7.29 mL, 160 mmol) were stirred at room temperature for 10–15 min. Starting compound **(3a** or **b)** (20 mmol) was added slowly to the stirred solution which was then heated at 140 °C for 10–12 h.

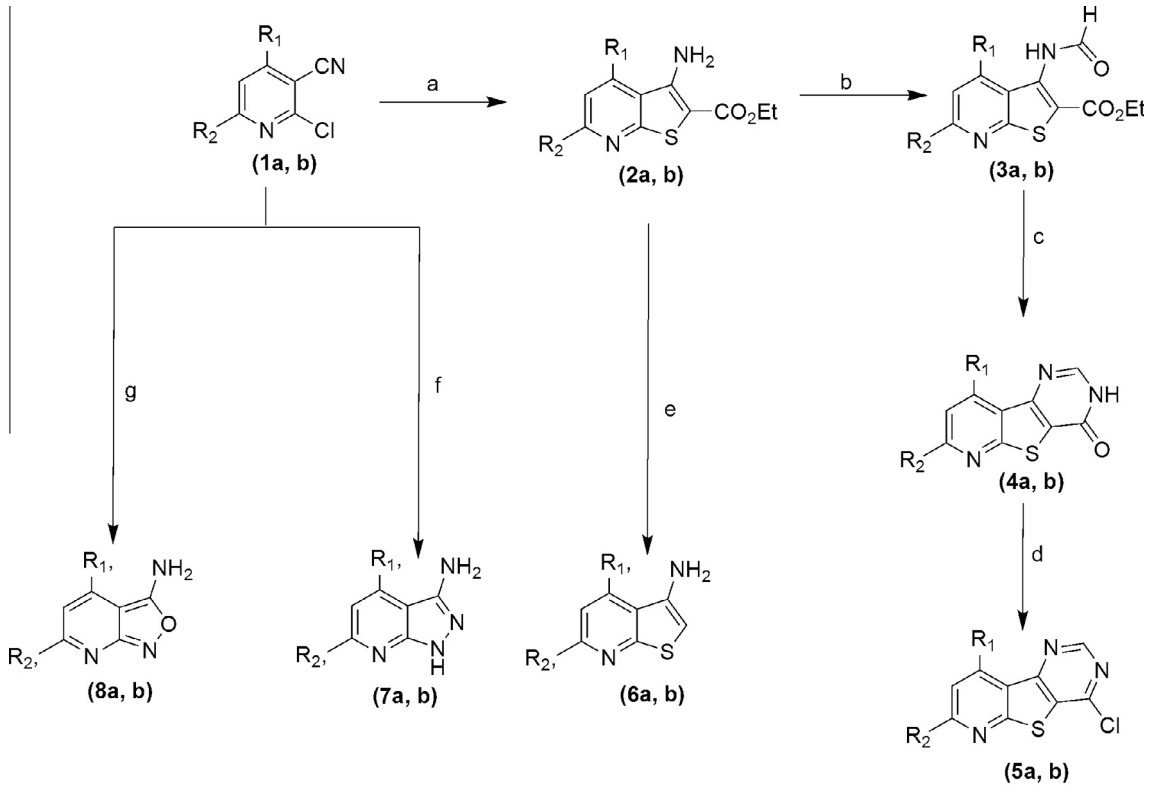

Scheme 1. Synthesis of intermediate compounds **(2a**, **b)**, **(3a**, **b)**, **(4a**, **b)**, **(5a**, **b)**, **(6a**, **b)**, **(7a**, **b)** and **(8a**, **b)**. Reagents and conditions: (a) Ethyl 2-mercaptoacetate, the appropriate base, dry ethanol, reflux, 4.5–6 h; (b) aqueous formic acid 85% v/v, toluene, reflux, 6–9 h; (c) ammonium formate, formamide, 140 °C, 10–12 h; (d) oxalyl chloride, reflux, 6–8 h; (e) 2 N NaOH, reflux, 2–4 h, oxalic acid, *iso*-propanol, 38 °C, 1–2 h; (f) hydrazine hydrate, *n*-butanol, reflux, 6–8 h; (g) hydroxylamine hydrochloride, dry THF, Et_3N, reflux, 6–8 h.

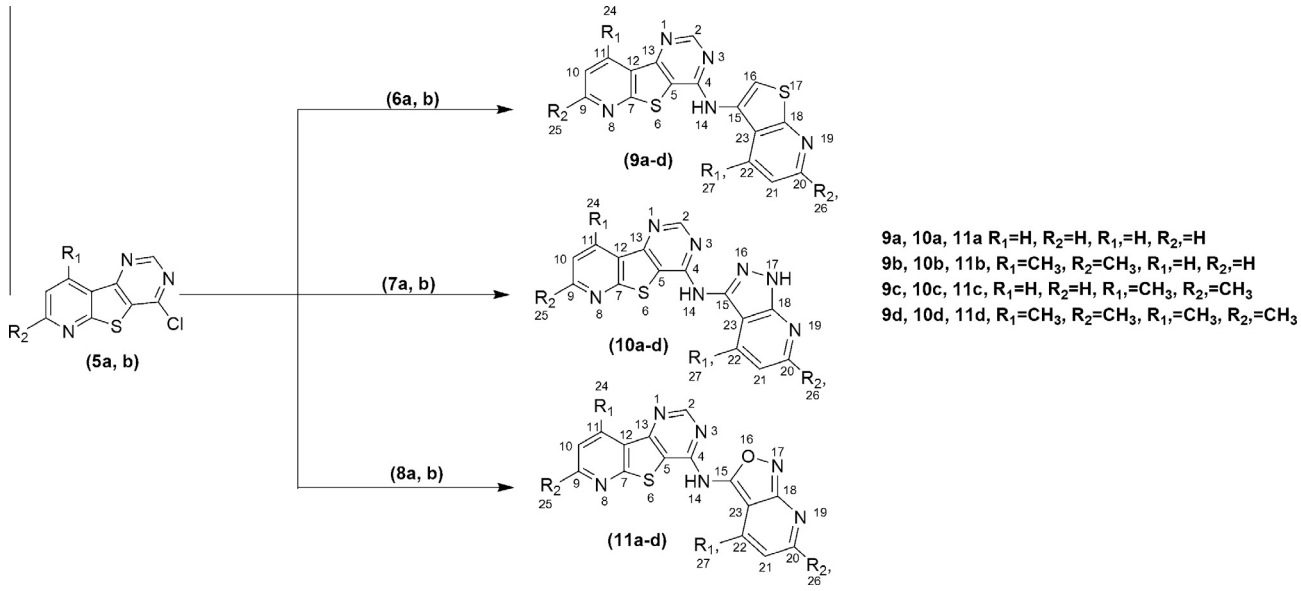

Scheme 2. Synthesis of targeted compounds **(9a–d)**, **(10a–d)** and **(11a–d)**. Reagents and conditions: Dry THF, Et_3N, reflux, 18–20 h.

After standing at room temperature, the precipitated solid was filtered, washed with cold water (2 × 5 mL) then dried in vacuum and recrystallised from ethanol [16].

*2.1.7. Pyrido[3′,2′:4,5]thieno[3,2-d]pyrimidin-4(3H)-one (**4a**)*

Long yellow needles; yield (3.6 g, 17.7 mmol, 72%); mp 272–273 °C [27].

*2.1.8. 7,9-Dimethylpyrido[3′,2′:4,5]thieno[3,2-d]pyrimidin-4(3H)-one (**4b**)*

Fine yellow crystals; yield (4.4 g, 19.2 mmol, 80%); mp 290–292 °C [28].

*2.1.9. General procedures adapted for the synthesis of 4-chloropyrido[3′,2′:4,5]thieno[3,2-d]pyrimidine derivatives (**5a**, **b**)*

The starting compound **(4a** or **b)** (10 mmol) and oxalyl chloride (10 mL) were heated to reflux for 6–8 h. The excess of oxalyl chloride was evaporated under reduced pressure and the resulting solid was taken to the next step without any further purification [29].

*2.1.10. 4-Chloropyrido[3′,2′:4,5]thieno[3,2-d]pyrimidine (**5a**)*

Brown powder; yield (1.3 g, 6.2 mmol, 68%); mp 153–155 °C [29].

*2.1.11. 7,9-Dimethyl-4-chloropyrido[3′,2′:4,5]thieno[3,2-d]pyrimidine (**5b**)*

Pale brown solid; yield (1.7 g, 6.9 mmol, 75%), mp 186–188 °C [28].

*2.1.12. General procedures adapted for the synthesis of 3-aminothieno[2,3-b]pyridine derivatives (**6a**, **b**)*

The starting compound **(2a** or **b)** (50 mmol) was dissolved in 2 N NaOH (160 mL) and the mixture was refluxed for 2–4 h. The solution was cooled to 0 °C and acidified to pH 1 with concentrated HCl. The resulting precipitate was collected by filtration. Oxalic acid (13.10 g, 100 mmol) was added to the solution of the crude product in *iso*-propanol (60 mL). The solution was stirred at 38 °C for 1–2 h. After standing at the room temperature, the mixture was cooled in an ice bath and diethyl ether (40 mL) was added. The white precipitate that formed was filtered and washed with diethyl ether (2 × 10 mL). The precipitate (5 mmol) was suspended in cold water (35 mL) and the pH was adjusted to 14 with aqueous NH_4OH solution (35% v/v). The solution was extracted with CH_2Cl_2 (4 × 100 mL). The organic layer was isolated and evaporated under reduced pressure. The resulting solid was recrystallised from THF [30].

*2.1.13. 3-Aminothieno[2,3-b]pyridine (**6a**)*

White crystals; yield (3.5 g, 23.6 mmol, 32%); mp 122–123 °C [31].

*2.1.14. 3-Amino-4,6-dimethylthieno[2,3-b]pyridine (**6b**)*

White crystals; yield (4.5 g, 25.2 mmol, 36%); mp 133–134 °C [32].

*2.1.15. General procedures for the synthesis of 3-aminopyrazolo[3,4-b]pyridine derivatives (**7a**, **b**)*

A mixture of starting compound **(1a** or **b)** (10 mmol) and hydrazine hydrate (30 mmol) was refluxed for 6–8 h in *n*-butanol (20 mL). The reaction mixture was left to cool in an ice bath at 0 °C, the precipitate was collected by filtration and recrystallised from methanol [33].

*2.1.16. 3-Aminopyrazolo[3,4-b]pyridine (**7a**)*

Yellow crystalline solid; yield (1.05 g, 7.8 mmol, 77%); mp 270–272 °C [34].

*2.1.17. 3-Amino-4,6-dimethylpyrazolo[3,4-b]pyridine (**7b**)*

Light yellow crystals; yield (1.3 g, 8.4 mmol, 82%); mp 280–281 °C [33].

*2.1.18. General procedures for the synthesis of 3-aminoisoxazolo[3,4-b]pyridine derivatives (**8a**, **b**)*

A mixture of starting compound **(1a** or **b)** (10 mmol) and hydroxylamine hydrochloride (10 mmol) was refluxed for 6–8 h in dry THF (20 mL) and Et_3N (3 mL). The reaction mixture was left to cool in an ice bath at 0 °C, the precipitate was filtered off and recrystallised from *o*-xylene [33].

*2.1.19. 3-Aminoisoxazolo[3,4-b]pyridine (**8a**)*

White crystalline solid; yield (1 g, 7.4 mmol, 73%); mp 210–211 °C [35].

*2.1.20. 3-Amino-4,6-dimethylisoxazolo[3,4-b]pyridine (**8b**)*

White crystalline solid; yield (1.2 g, 7.5 mmol, 74%); mp 252–253 °C [33].

*2.1.21. General procedures for the synthesis of pyrido[3′,2′:4,5]thieno[3,2-d]pyrimidin-4-amines (**9a–d**), (**10a–d**) and (**11a–d**)*

The appropriate starting amino compound **(6a**, **b)**, **(7a**, **b)** and **(8a**, **b)** (9 mmol) was dissolved in dry THF (25 mL) and Et_3N (1 mL) under nitrogen atmosphere. Compound (**5a** or **b**) (4 mmol) was added slowly to the stirred solution then heated under reflux for 18–20 h. The reaction mixture was concentrated under reduced pressure. The residue was dissolved in EtOAc and washed with 1 M aqueous K_2CO_3 solution (3 × 15 mL). The organic layer was then dried over Na_2SO_4, filtered and concentrated in vacuum. The residue was purified by column chromatography eluting with 1–3 EtOAc/hexane v/v.

*2.1.22. N-(thieno[2,3-b]pyridine)pyrido[3′,2′:4,5]thieno[3,2-d]pyrimidin-4-amine (**9a**)*

Yield (0.3 g, 1 mmol, 41%); mp 235–236 °C. ^{1}H NMR (400 MHz, DMSO-d_6): δ 10.20 (1H, s, exch with D_2O, NH), 8.81 (2H, d, ^3J 4.80, H-9, H-20), 8.58 (2H, d, ^3J 7.60, H-11, H-22), 8.38 (2H, s, H-2, H-16), 7.64 (2H, t, ^3J 8.00, H-10, H-21); ^{13}C NMR (100 MHz, DMSO-d_6): δ 160.90 (C-7, C-18), 155.43 (C-4), 155.40 (C-2), 150.00 (C-13), 143.96 (C-9, C-20), 138.99 (C-15), 132.95 (C-11, C-22), 127.35 (C-12, C-23), 123.28 (C-21), 123.19 (C-10), 112.33 (C-5), 112.30 (C-16); IR (KBr): 3253 (N–H), 3044 (C–H, sp^2), 1618 (C=C, sp^2), 1449 (C=N) cm^{-1}; MS (EI): m/z 335.85 (M$^+$, 1.10%). Anal. Calcd for $C_{16}H_9N_5S_2$: C, 57.30; H, 2.70; N, 20.88. Found: C, 57.70; H, 3.02; N, 21.26.

*2.1.23. N-(thieno[2,3-b]pyridine)-7,9-dimethylpyrido[3′,2′:4,5]thieno-[3,2-d]pyrimidin-4-amine (**9b**)*

Yield (0.4 g, 1.2 mmol, 44%); mp 266–268 °C. ^{1}H NMR (300 MHz, DMSO-d_6): δ 11.79 (1H, s, exch with D_2O, NH), 8.39 (1H, d, ^3J 4.80, H-20), 7.68 (1H, t, ^3J 8.10, H-21), 7.07 (1H, d, ^3J 7.80, H-22), 6.68 (3H, s, H-2, H-10, H-16), 2.89 (6H, s, $(CH_3)_2$); ^{13}C NMR (100 MHz, DMSO-d_6): δ 160.29 (C-7, C-18), 156.06 (C-4, C-2), 150.43 (C-9), 145.37 (C-20), 144.22 (C-13), 138.07 (C-11, C-15), 133.59 (C-22), 129.23 (C-21), 123.96 (C-10), 121.42 (C-12, C-23), 109.99 (C-5, C-16), 23.98 (CH_3), 19.02 (CH_3); IR (KBr): 3432 (N–H), 2877 (C–H, sp^3), 1607 (C=C, sp^2), 1471 (C=N) cm^{-1}; MS (EI): m/z 367 (M$^+$+4, 1.23%), 231 (100%). Anal. Calcd for $C_{18}H_{13}N_5S_2$: C, 59.48; H, 3.61; N, 19.27. Found: C, 59.73; H, 3.72; N, 19.57.

*2.1.24. N-(4,6-dimethylthieno[2,3-b]pyridine)pyrido[3′,2′:4,5]thieno-[3,2-d]pyrimidin-4-amine (**9c**)*

Yield (0.3 g, 1 mmol, 43%); mp 266–267.5 °C. ^{1}H NMR (400 MHz, DMSO-d_6): δ 10.89 (1H, s, exch with D_2O, NH), 7.75 (1H, d, ^3J 4.80, H-9), 7.18 (1H, d, ^3J 7.60, H-11), 6.87 (2H, s, H-2, H-16), 6.45 (1H, t, ^3J 8.00, H-10), 6.15 (1H, s, H-21), 2.31 (3H, s, CH_3), 2.28 (3H, s, CH_3); ^{13}C NMR (100 MHz, DMSO-d_6): δ 160.96 (C-7, C-18), 154.67 (C-4, C-2), 152.06 (C-20), 150.87 (C-13), 145.91 (C-9), 142.34 (C-22), 136.80 (C-15), 131.90 (C-11), 128.37 (C-10), 124.28 (C-21), 120.92 (C-12, C-23), 113.40 (C-5, C-16), 22.00 (CH_3), 18.14 (CH_3); IR (KBr): 2887 (C–H, sp^3), 1662 (C=C, sp^2), 1440 (C=N) cm^{-1}; MS (EI): m/z 363.00 (M$^+$, 10.11%). Anal. Calcd for $C_{18}H_{13}N_5S_2$: C, 59.48; H, 3.61; N, 19.27. Found: C, 59.71; H, 3.80; N, 19.63.

*2.1.25. N-(4,6-dimethylthieno[2,3-b]pyridine)-7,9-dimethylpyrido-[3′,2′:4,5]thieno[3,2-d]pyrimidin-4-amine (**9d**)*

Yield (0.4 g, 1.2 mmol, 50%); mp 296–298 °C. ^{1}H NMR (400 MHz, DMSO-d_6): δ 12.87 (1H, s, exch with D_2O, NH), 8.32 (1H, s, H-2), 7.24 (1H, s, H-16), 6.44 (2H, s, H-10, H-21), 2.83 (6H, s, $(CH_3)_2$), 2.56 (6H, s, $(CH_3)_2$); ^{13}C NMR (100 MHz, DMSO-d_6): δ 160.22 (C-7, C-18), 155.32 (C-4, C-2), 152.43 (C-13, C-9, C-20), 141.47 (C-11, C-22), 135.02 (C-15), 130.23 (C-10, C-21), 123.77 (C-16), 117.30 (C-12, C-5, C-23), 24.09 $(CH_3)_2$, 18.13 $(CH_3)_2$; IR (KBr): 2989 (C–H, sp^3), 1664 (C=C, sp^2), 1546 (C=N) cm^{-1}; MS (EI): m/z 392.00 (M$^+$+1, 38.72%), 231 (100%). Anal. Calcd for $C_{20}H_{17}N_5S_2$: C, 61.36; H, 4.38; N, 17.89. Found: C, 61.58; H, 4.55; N, 18.24.

*2.1.26. N-(pyrazolo[3,4-b]pyridine)pyrido[3′,2′:4,5]thieno[3,2-d]pyrimidin-4-amine (**10a**)*

Yield (0.2 g, 0.8 mmol, 32%); mp 300 °C. ^{1}H NMR (400 MHz, DMSO-d_6): δ 9.49 (2H, s, exch with D_2O, NH), 8.79 (2H, dd, ^3J 4.80, ^4J 2.00, H-9, H-20), 8.29 (1H, s, H-2), 8.11 (2H, dd, ^3J 8.00, ^4J 2.00, H-11, H-22), 7.70 (2H, t, ^3J 8.00, H-10, H-21); ^{13}C NMR (100 MHz, DMSO-d_6): δ 163.34 (C-7, C-15), 160.46 (C-4, C-2, C-18), 152.87 (C-13), 140.21 (C-9, C-20), 131.99 (C-11, C-22), 128.20 (C-12, C-23), 121.80 (C-10, C-21), 116.11 (C-5); IR (KBr): 3441 (N–H), 1679 (C=C, sp^2), 1476 (C=N) cm^{-1}; MS (EI): m/z 320.20 (M$^+$+1, 0.20%). Anal. Calcd for $C_{15}H_9N_7S$: C, 56.42; H, 2.84; N, 30.70. Found: C, 56.27; H, 2.58; N, 30.48.

*2.1.27. N-(pyrazolo[3,4-b]pyridine)-7,9-dimethylpyrido[3′,2′:4,5]thieno[3,2-d]pyrimidin-4-amine (**10b**)*

Yield (0.3 g, 1 mmol, 36%); mp > 300 °C (decomp.). ^{1}H NMR (300 MHz, DMSO-d_6): δ 11.79 (1H, s, exch with D_2O, NH), 8.63 (1H, s, H-2), 8.46 (1H, d, ^3J 4.80, H-20), 7.92 (1H, d, ^3J 8.40, H-22), 7.21 (1H, t, ^3J 8.10, H-21), 6.78 (1H, s, H-10), 4.10 (1H, s, exch with D_2O, NH), 2.89 (3H, s, CH_3), 2.60 (3H, s, CH_3); ^{13}C NMR (100 MHz, DMSO-d_6): δ 161.33 (C-15), 157.48 (C-4, C-2), 157.46 (C-7, C-18), 151.58 (C-9), 151.56 (C-13), 146.57 (C-11), 142.22 (C-20), 131.99 (C-22), 128.20 (C-21), 122.30 (C-10), 121.20 (C-12, C-23), 119.15 (C-5), 24.03 (CH_3), 18.92 (CH_3); IR (KBr): 3205 (N–H), 3025 (C–H, sp^2), 2855 (C–H, sp^3), 1633 (C=C, sp^2), 1548 (C=N) cm^{-1}; MS (EI): m/z 349.00 (M$^+$+2, 0.77%), 231 (100%). Anal. Calcd for $C_{17}H_{13}N_7S$: C, 58.77; H, 3.77; N, 28.22. Found: C, 58.62; H, 3.50; N, 28.00.

*2.1.28. N-(4,6-dimethylpyrazolo[3,4-b]pyridine)pyrido[3′,2′:4,5]thieno[3,2-d]pyrimidin-4-amine (**10c**)*

Yield (0.3 g, 0.9 mmol, 39%); mp > 300 °C (decomp.). ^{1}H NMR (400 MHz, DMSO-d_6): δ 12.28 (1H, s, exch with D_2O, NH), 11.74 (1H, s, exch with D_2O, NH), 8.80 (1H, d, ^3J 4.80, H-9), 8.43 (1H, d, ^3J 8.00, H-11), 7.54 (1H, t, ^3J 8.00, H-10), 6.53 (2H, s, H-2, H-21), 1.62 (3H, s, CH_3), 1.29 (3H, s, CH_3); ^{13}C NMR (100 MHz, DMSO-d_6): δ 164.33 (C-15), 157.46 (C-2, C-7), 157.44 (C-4, C-18), 151.24 (C-20), 151.22 (C-13), 148.30 (C-22), 142.22 (C-9), 131.99 (C-11), 128.20 (C-12, C-10, C-23), 122.30 (C-21), 117.46 (C-5), 24.12 (CH_3), 20.63 (CH_3); IR (KBr): 3388 (N–H), 2883 (C–H, sp^3), 1647 (C=C, sp^2) cm^{-1}; MS (EI): m/z 347.80 (M$^+$, 0.60%). Anal. Calcd for $C_{17}H_{13}N_7S$: C, 58.77; H, 3.77; N, 28.22. Found: C, 58.89; H, 4.00; N, 28.62.

*2.1.29. N-(4,6-dimethylpyrazolo[3,4-b]pyridine)-7,9-dimethylpyrido[3′,2′:4,5]thieno[3,2-d]pyrimidin-4-amine (**10d**)*

Yield) 0.4 g, 1.2 mmol, 45%); mp > 300 °C (decomp.). ^{1}H NMR (400 MHz, DMSO-d_6): δ 12.91 (1H, s, exch with D_2O, NH), 8.35 (1H, s, H-2), 7.29 (2H, s, H-10, H-21), 5.75 (1H, s, exch with D_2O, NH), 2.80 (3H, s, CH_3), 2.58 (9H, s, $(CH_3)_3$); ^{13}C NMR (100 MHz, DMSO-d_6): δ 165.19 (C-15), 159.42 (C-4, C-2, C-18), 159.39 (C-9, C-7, C-20), 158.33 (C-13), 144.97 (C-11, C-22), 123.75 (C-12, C-23), 123.27 (C-10, C-21), 112.80 (C-5), 23.98 (CH_3), 18.99 (CH_3),

15.05 (CH_3)$_2$; IR (KBr): 3421 (N–H), 2976 (C–H, sp^3), 1677 (C=C, sp^2), 1476 (C=N) cm^{-1}; MS (EI): m/z 375.00 (M^+, 44.81%). Anal. Calcd for $C_{19}H_{17}N_7S$: C, 60.78; H, 4.56; N, 26.11. Found: C, 61.03; H, 4.89; N, 26.33.

*2.1.30. N-(isoxazolo[3,4-b]pyridine)pyrido[3′,2′:4,5]thieno[3,2-d]pyrimidin-4-amine (**11a**)*

Yield) 0.3 g, 0.9 mmol, 36%); mp 262–264 °C. ^{1}H NMR (400 MHz, DMSO-d_6): δ 11.33 (1H, s, exch with D_2O, NH), 8.78 (2H, d, ^3J 5.20, H-9, H-20), 8.43 (2H, d, ^3J 8.00, H-11, H-22), 7.66 (1H, s, H-2), 7.34 (2H, t, ^3J 8.00, H-10, H-21); ^{13}C NMR (100 MHz, DMSO-d_6): δ 160.92 (C-15), 154.49 (C-4, C-2, C-7, C18), 150.03 (C-13), 144.97 (C-9, C-20), 132.91 (C-11, C-22), 123.73 (C-10, C-21), 123.20 (C-12, C-23), 112.17 (C-5); IR (KBr): 3047 (C–H, sp^2), 1681 (C=C, sp^2), 1523 (C=N) cm^{-1}; MS (EI): m/z 320.20 (M^+, 1.18%). Anal. Calcd for $C_{15}H_8N_6OS$: C, 56.24; H, 2.52; N, 26.24. Found: C, 56.00; H, 2.12; N, 26.10.

*2.1.31. N-(isoxazolo[3,4-b]pyridine)-7,9-dimethylpyrido[3′,2′:4,5]thieno[3,2-d] pyrimidin-4-amine (**11b**)*

Yield) 0.3 g, 1.1 mmol, 40%); mp 270–271 °C. ^{1}H NMR (400 MHz, DMSO-d_6): δ 8.81 (1H, d, ^3J 4.80, H-20), 8.79 (1H, s, H-2), 8.43 (1H, d, ^3J 8.00, H-22), 7.32 (1H, s, H-10), 6.99 (1H, t, ^3J 8.00, H-21), 5.75 (1H, s, exch with D_2O, NH), 2.61 (3H, s, CH_3), 2.57 (3H, s, CH_3); ^{13}C NMR (100 MHz, DMSO-d_6): δ 161.33 (C-15), 159.71 (C-7), 157.48 (C-4, C-2, C-18), 152.43 (C-13, C-9), 147.18 (C-11), 146.83 (C-20), 132.91 (C-22), 126.93 (C-21), 124.28 (C-10), 123.27 (C-12, C-23), 113.83 (C-5), 22.05 (CH_3), 18.20 (CH_3); IR (KBr): 3438 (N–H), 2985 (C–H, sp^3), 1645 (C=C, sp^2), 1475 (C=N) cm^{-1}; MS (EI): m/z 348.90 (M^+, 0.55%), 231 (100%). Anal. Calcd for $C_{17}H_{12}N_6OS$: C, 58.61; H, 3.47; N, 24.12. Found: C, 58.23; H, 3.32; N, 23.93.

*2.1.32. N-(4,6-dimethylisoxazolo[3,4-b]pyridine)pyrido[3′,2′:4,5]thieno[3,2-d]pyrimidin-4-amine (**11c**)*

Yield (0.3 g, 1 mmol, 42%); mp 269–271 °C. ^{1}H NMR (400 MHz, DMSO-d_6): δ 12.31 (1H, s, exch with D_2O, NH), 8.51 (1H, d, ^3J 4.80, H-9), 8.43 (1H, d, ^3J 8.00, H-11), 7.59 (1H, t, ^3J 8.00, H-10), 6.61 (1H, s, H-2), 6.13 (1H, s, H-21), 2.31 (3H, s, CH_3), 2.28 (3H, s, CH_3); ^{13}C NMR (100 MHz, DMSO-d_6): δ 164.06 (C-15), 163.57 (C-7), 157.46 (C-4, C-2, C-18), 152.87 (C-20), 151.24 (C-13), 148.21 (C-22), 142.22 (C-9), 132.99 (C-11), 124.06 (C-12, C-23), 122.71 (C-10), 121.16 (C-21), 116.18 (C-5), 20.60 (CH_3), 18.95 (CH_3); IR (KBr): 2857 (C–H, sp^3), 1690 (C=C, sp^2), 1455 (C=N) cm^{-1}; MS (EI): m/z 348.20 (M^+, 0.71%). Anal. Calcd for $C_{17}H_{12}N_6OS$: C, 58.61; H, 3.47; N, 24.12. Found: C, 58.86; H, 3.80; N, 24.40.

*2.1.33. N-(4,6-dimethylisoxazolo[3,4-b]pyridine)-7,9-dimethylpyrido[3′,2′:4,5]thieno[3,2-d] pyrimidin-4-amine (**11d**)*

Yield (0.4 g, 1.1 mmol, 44%); mp > 300 °C (decomp.). ^{1}H NMR (400 MHz, DMSO-d_6): δ 12.31 (1H, s, exch with D_2O, NH), 6.18 (3H, s, H-2, H-10, H-21), 2.28 (6H, s, (CH_3)$_2$), 2.24 (6H, s, (CH_3)$_2$); ^{13}C NMR (100 MHz, DMSO-d_6): δ 161.33 (C-7, C-15), 157.46 (C-4, C-2, C-18), 152.51 (C-13, C-9, C-20), 147.16 (C-11, C-22), 124.19 (C-10, C-21), 122.74 (C-12, C-23), 110.70 (C-5), 24.03 (CH_3)$_2$, 18.99 (CH_3)$_2$; IR (KBr): 2885 (C–H, sp^3), 1660 (C=C, sp^2), 1548 (C=N) cm^{-1}; MS (EI): m/z 376.00 (M^+, 19.22%). Anal. Calcd for $C_{19}H_{16}N_6OS$: C, 60.62; H, 4.28; N, 22.33. Found: C, 60.92; H, 4.56; N, 22.60.

2.2. Biological evaluation

2.2.1. Protein kinase inhibitory assays

The protein kinase inhibitory assays were carried out by BPS Bioscience at single dose concentration of 10 μM [36]. VEGFR-1/Flt1 (BPS#40223), VEGFR-2/KDR (BPS#40301), EGFR (BPS#40187), CDK5/p25 (BPS#40105), GSK3α (BPS#40006), GSK3β (BPS#40007) served as enzymes sources. While GSKtide (BPS), Histone H1 (NEB#M2501S), Poly (Glu, Tyr) sodium salt, (4:1, Glu:Tyr) (Sigma#P7244) served as the standardized substrate, in addition to kinase-GloTM plus luminescence kinase assay kit (Promega#V3772) and ADP-GloTM kinase assay kit (Promega#V9101). 33P-ATP was purchased from Perkin Elmer and ADP-GloTM was purchased from Promega. All other materials were of standard laboratory grade.

2.2.1.1. Assay protocols. The assays for VEGFR-2/KDR, EGFR, CDK5/p25, GSK3α and GSK3β were performed using kinase-GloTM plus luminescence kinase assay kit (Promega#V3772). It measures kinase activity by quantitating the amount of ATP remaining in solution following a kinase reaction. The luminescent signal obtained from the assay is correlated with the amount of ATP present and is inversely correlated with the kinase activity. The compounds were diluted in 10% DMSO and 5 μL of the dilution was added to a 50 μL reaction so that the final concentration of DMSO was 1% in all of reactions. All of the enzymatic reactions were conducted at 30 °C for 40 min. The 50 μL reaction mixture contains 40 mM Tris, pH 7.4, 10 mM $MgCl_2$, 0.1 mg/mL BSA, 1 mM DTT, 10 μM ATP, kinase substrate and the enzyme. After the enzymatic reaction, 50 μL of kinase-GloTM plus luminescence kinase assay solution (Promega#V3772) was added to each reaction and the plate was incubated for 5 min at room temperature. Luminescence signal was measured using Tecan Infinite M1000 microplate reader. The assay for VEGFR-1/Flt1 was performed using ADP-GloTM kinase assay reagents (Promega#V9101). It measures kinase activity by quantitating the ADP amount produced from the enzymatic reaction. The luminescent signal from the assay is correlated with the amount of ADP present and is directly correlated with the kinase activity. Other conditions were the same as the previous procedures, except the final reaction volume was reduced to 25 μL. After the 40 min kinase reaction at 30 °C, 25 μL of ADP-GloTM reagent was added and incubated for 45 min at room temperature followed by another 50 min incubation with 50 μL of kinase detection mixture. Luminescence signal was measured using a Tecan Infinite M1000 microplate reader [36].

The protein kinase assays used to determine IC_{50} value were performed using ADP-GloTM assay kit from Promega which measures the generation of ADP by the protein kinase. Generation of ADP by the protein kinase reaction leads to an increase in luminescence signal in the presence of ADP-GloTM assay kit. The assay was started by incubating the reaction mixture in a 96-well plate at 30 °C for 30 min. After the 30 min incubation period, the assay

Table 1
Summary of the % inhibitory effects of targeted compounds **(9a–d)**, **(10a–d)** and **(11a–d)** on protein kinase activity.

Compound	VEGFR-1 (Flt-1)	VEGFR-2 (KDR)	EGFR	CDK5/p25	GSK3α	GSK3β
9a	NA[a]	21[b]	NA	NA	NA	NA
9b	NA	40	NA	NA	NA	NA
9c	40	47	11	20	6	12
9d	44	67	7	32	NA	NA
10a	NA	11	NA	NA	NA	NA
10b	NA	20	NA	NA	NA	NA
10c	NA	13	NA	NA	NA	NA
10d	NA	12	NA	NA	NA	NA
11a	NA	6	NA	NA	NA	NA
11b	NA	11	NA	NA	NA	NA
11c	NA	11	NA	NA	NA	NA
11d	NA	18	NA	NA	NA	NA
Staurosporine	86[c]	99	97	100	96	98

[a] NA: Not active.
[b] % Inhibition values of compounds on the protein kinase activity at 10 μM.
[c] % Inhibition values of Staurosporine on the protein kinase activity at 100 nM.

was terminated by the addition of 25 mL of ADPGloTM Reagent (Promega). The 96-well plate was shaken and then incubated for 40 min at ambient temperature, 50 mL of kinase detection reagent was added, the 96-well reaction plate was then read using the ADP-GloTM luminescences protocol on a GloMaxTM plate reader (Promega: Catalog #E7031). Blank control was set up that included all the assay components except the addition of appropriate substrate (replace with equal volume of kinase assay buffer). The corrected activity for each protein kinase target was determined by removing the blank control value [36].

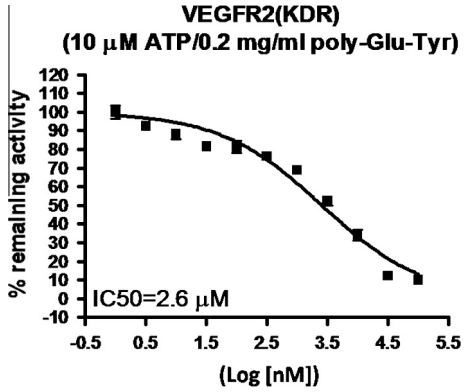

Fig. 2. Graph of compound **(9d)** shows log inhibitor concentration against activity of human VEGFR-2.

2.2.1.2. Data analysis. Kinase activity assays were performed in duplicate at each concentration. The luminescence data was analysed using the computer software, graph pad Prism. The difference between luminescence intensities in the absence of kinase (Lut) and in the presence of kinase (Luc) was defined as 100% activity (Lut − Luc). Using luminescence signal (Lu) in the presence of the compound, % activity was calculated as: % activity = [(Lut − Lu)/(Lut − Luc)] × 100%, where Lu = the luminescence intensity in the presence of the compound (all percent activities below zero were set to 0%). % Inhibition was calculated as: % inhibition = 100 (%) − % activity [36].

2.2.1.3. Measurement of potential enzyme inhibitory activity IC_{50}. IC_{50} value for compound **(9d)** against VEGFR-2/KDR was estimated by

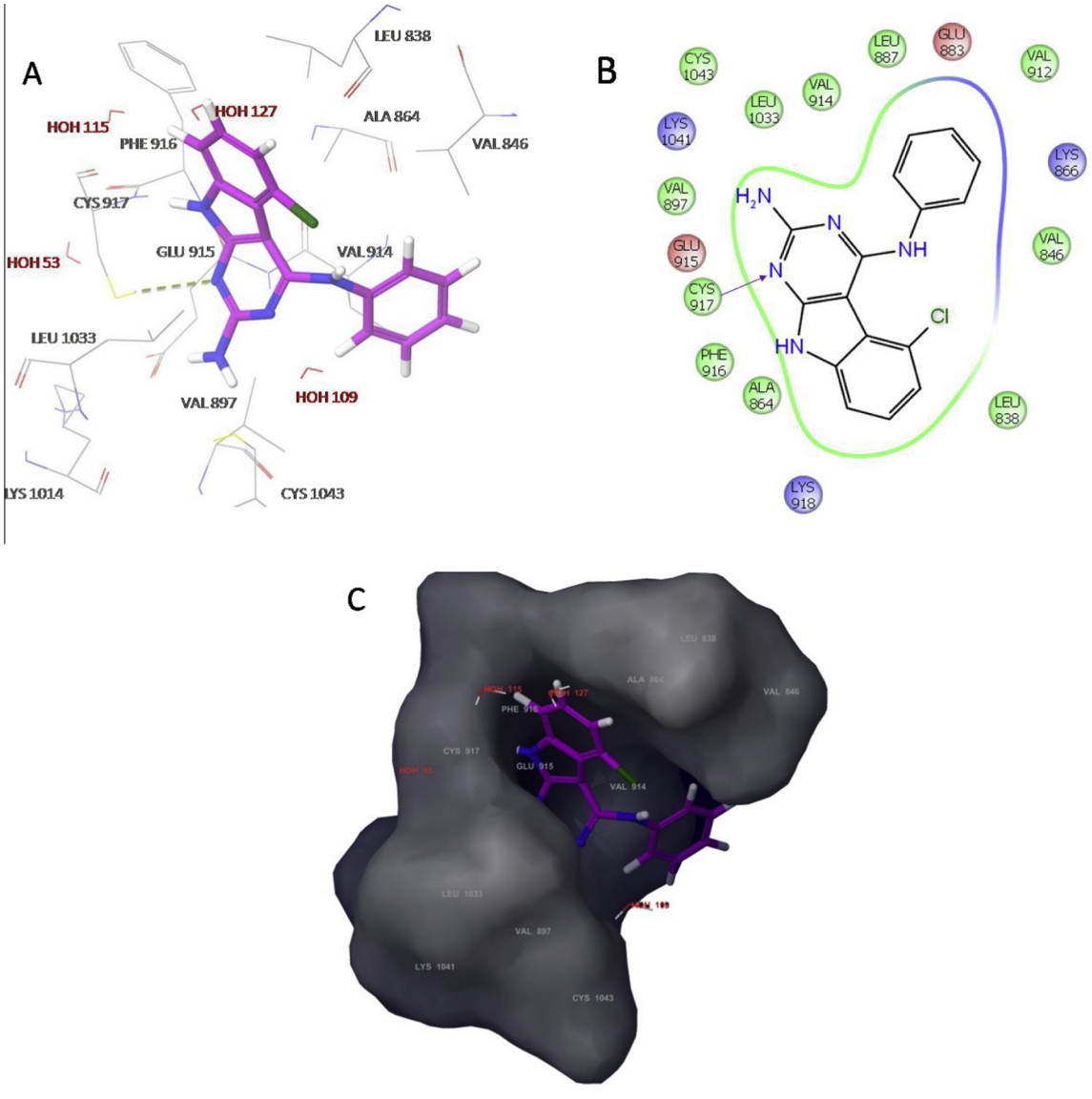

Fig. 3. Docking of 5-chloro-*N*-phenyl-9*H*-pyrimido[4,5-*b*]indole-2,4-diamine in the kinase binding domain of VEGFR-2 (PDB code: 1YWN).

generating a graph of log inhibitor versus normalized response with variable using the prism software [36].

2.3. Molecular modelling

Molecular modelling was carried out on Schrodinger computational software workstation using Maestro 9.3 graphic user interface (GUI). The atomic coordinates and the cartesian matrix of the polypeptide were obtained from the protein bank database PDB (Brookhaven protein database 1YWN). The basic and acidic amino acids were neutralized at pH 7 ± 2 by protonation of the terminal amino groups of basic amino acids and the terminal carboxylic acid groups of acidic amino acids were deprotonated. The docking process involved the standard precision docking (SP) in which ligand poses that scored bad energies would be rejected. Partial charge cut-off was set to 0.25 for the receptor and 0.15 for the ligand to soften the potential of non-polar parts. Flexible docking was performed with no torsional constraints was applied. Twenty percent of the final poses produced from the SP docking were subjected to the Extra Precision mode of Glide docking (XP) to perform strict and more precise docking simulation. Aromatic rings were forbidden to flip and amide bonds of the polypeptide segments with non-polar amide bonds were penalized [37].

3. Results and discussion

3.1. Chemistry

The Thorpe–Ziegler cyclization procedure was adapted for the synthesis of 3-aminothieno[2,3-*b*]pyridine-2-ethyl carboxylate derivatives **(2a**, **b)** in high yields 87–95% [23,24]. The synthesis of 3-formylaminothieno[2,3-*b*]pyridine derivatives **(3a**, **b)** involved the reaction of compounds **(2a**, **b)** with formic acid in toluene [25]. Pyrido[3′,2′:4,5]thieno[3,2-*d*]pyrimidin-4-one derivatives **(4a**, **b)** were obtained through simple cyclization of compounds **(3a**, **b)** with ammonium formate in formamide [16]. Treatment of pyrido[3′,2′:4,5]thieno[3,2-*d*]pyrimidin-4-one derivatives **(4a**, **b)** with oxalyl chloride has given 4-chloropyrido[3′,2′:4,5]thieno-[3,2-*d*]pyrimidine derivatives **(5a**, **b)** [29]. 3-Aminothieno[2,3-*b*]-pyridine derivatives **(6a**, **b)** were accessible through the same intermediates **(2a**, **b)** used in the preparation of pyrido[3′,2′:4,5]thieno[3,2-*d*]pyrimidin-4-one derivatives **(4a**, **b)**. The reaction involved the hydrolysis of compounds **(2a**, **b)** with 2 N sodium hydroxide solution followed by decarboxylation of the free carboxylic acid intermediates to afford the corresponding free amines **(6a**, **b)** (Scheme 1) [30]. Furthermore, the reaction of hydrazine hydrate and hydroxylamine hydrochloride with 2-chloro-3-cyanopyridine derivatives **(1a**, **b)** has afforded 3-

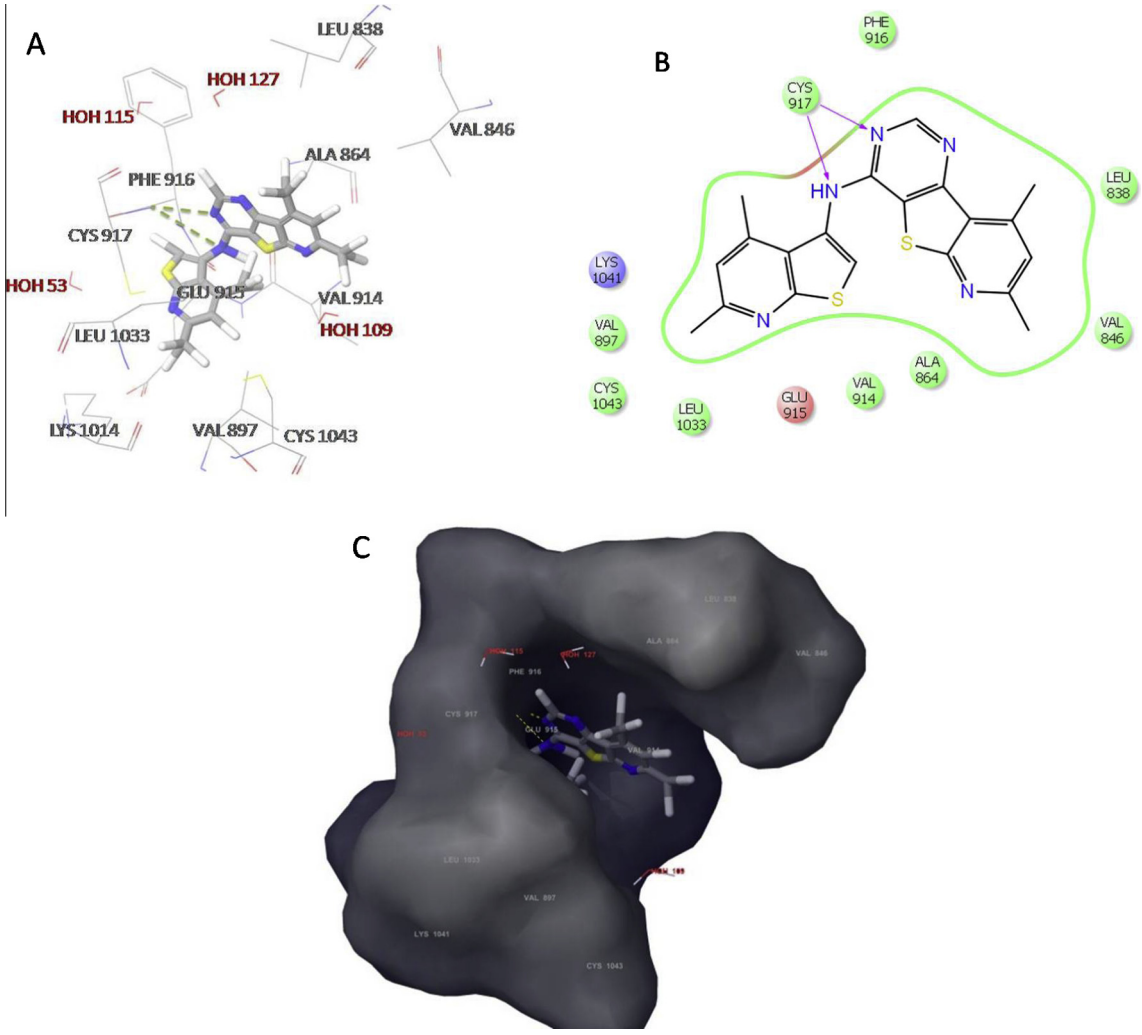

Fig. 4. Docking of compound (**9d**) in the kinase binding domain of VEGFR-2 (PDB code: 1YWN).

aminopyrazolo[3,4-*b*]pyridine derivatives **(7a, b)** and 3-aminoisoxazolo[3,4-*b*]pyridine derivatives **(8a, b)**, respectively [33]. Finally, 4-chloropyrido[3′,2′:4,5]thieno[3,2-*d*]pyrimidine derivatives **(5a, b)** were allowed to react with the respective heteroaryl amines **(6a, b)**, **(7a, b)** and **(8a, b)** to afford target compounds **(9a–d)**, **(10a–d)** and **(11a–d)** (Scheme 2).

The structures of the synthesized compounds **(9a–d)**, **(10a–d)** and **(11a–d)** were elucidated by elemental analyses and spectral data (IR, ^{1}H NMR, ^{13}C NMR and EI-MS). IR spectra showed collectively secondary amine signals at around 3300–3500 cm^{-1} pertaining to the coupling between 4-chloropyrido[3′,2′:4,5]thieno[3,2-*d*]pyrimidine derivatives **(5a, b)** and the primary heteroaryl amines **(6a, b)**, **(7a, b)** and **(8a, b)**. ^{1}H NMR spectra of the target compounds **(9a–d)**, **(10a–d)** and **(11a–d)** were characterized by four aromatic protons displayed downfield. The H-2 proton of the pyrimidine ring appeared as a singlet (s) peak at 7.66–8.38 ppm. While the protons of the pyridine ring occasionally appeared either as doublets of doublets (dd) or doublets (d) at 8.78–8.81 ppm corresponding to H-9 and triplets (t) at 7.64–7.70 ppm corresponding to H-10 and doublets of doublets (dd) or doublets (d) at 8.11–8.58 ppm corresponding to H-11. Moreover, compounds **(9b–d)**, **(10b–d)** and **(11b–d)** were characterized by singlets (s) corresponding to CH_3 protons displayed upfield at 1.29–2.89 ppm. ^{13}C NMR spectra showed signals for the pyrido[3′,2′:4,5]thieno[3,2-*d*]pyrimidine, isoxazolo[3,4-*b*]pyridine, pyrazolo[3,4-*b*]pyridine and thieno[2,3-*b*]pyridine rings at the expected chemical shifts.

3.2. Biological evaluation

3.2.1. Protein kinase inhibitory assays

The protein kinase inhibitory assays were performed at BPS Bioscience laboratories [36]. In the initial screening assay, compounds **(9a–d)**, **(10a–d)** and **(11a–d)** were tested at a single dose concentration 10 μM over a panel of 6 protein kinases. VEGFR-1/Flt-1 (BPS#40223), VEGFR-2/KDR (BPS#40301) and EGFR (BPS#40187) are tyrosine kinases. CDK5/p25 (BPS#40105), GSK3α (BPS#40006) and GSK3β (BPS#40007) are serine/threonine kinases. Staurosporine, a non selective ATP-competitive multikinase inhibitor, is considered as a reference compound [38].

Compound (**9d**) showed a selective kinase inhibitory profile against VEGFR-2 tyrosine kinase with an inhibition of 67% at 10 μM, whilst the inhibitory activities against the other 5 kinases were below 50%. The percentages of VEGFR-2 inhibition exerted by compounds **(9a–c)**, **(10a–d)** and **(11a–d)** were below 50% (Table 1).

Generally, thienopyridine analogues exhibited higher VEGFR-2 inhibitory activities when compared to pyrazolo and isoxazolopyridines (compare **9d**, **10d** and **11d**). The presence of hydrophobic methyl groups positioned at carbons 4 and 6 of the thienopyridine moiety represents another feature that enhanced greatly the inhibitory activity (compare **9a** and **9c**). Furthermore, substitutions with two hydrophobic methyl groups at the positions 7 and 9 of pyrido[3′,2′:4,5]thieno[3,2-*d*]pyrimidine core improved the activity and gave the most active compound in the study **(9d)**.

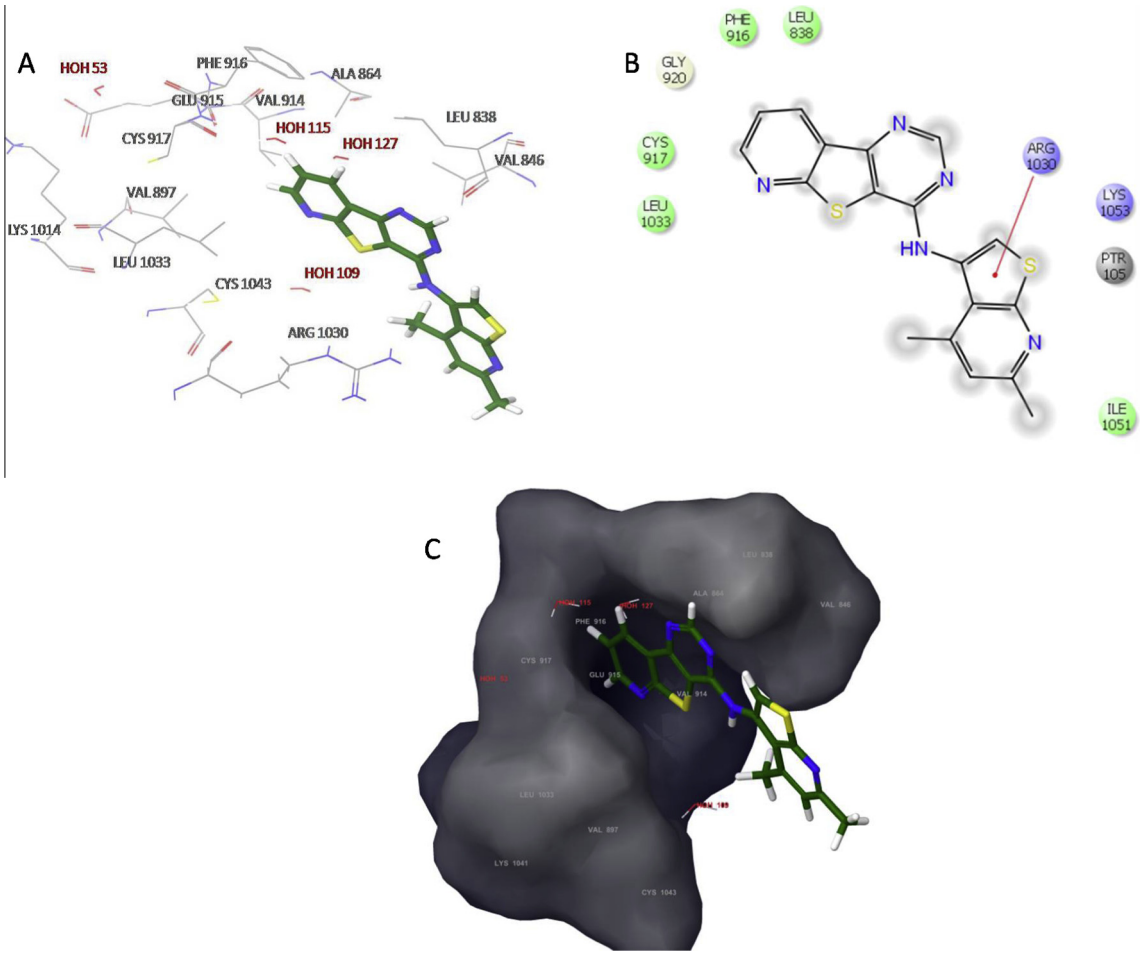

Fig. 5. Docking of compound (**9c**) in the kinase binding domain of VEGFR-2 (PDB code: 1YWN).

3.2.2. Measurement of potential enzyme inhibitory activity IC_{50}

The profiling data for compound **(9d)** against VEGFR-2 showed an increased inhibition of VEGFR-2 activity with increasing the concentration of compound **(9d)** (Fig. 2). This compound inhibited VEGFR-2 activity by 67% at the concentration 10 μM. The IC_{50} value for compound **(9d)** was 2.6 μM. This selective inhibition with a low micromolar range is considered a promising starting step for this new anti-VEGFR-2/KDR scaffold [39].

3.3. Ligand–receptor interaction studies of VEGFR-2 kinase inhibitors

Molecular docking was performed on the crystal structure of VEGFR-2 (PDB code 1YWN) [40]. The ligands used in this docking studies contain some structural resemblance to the reference compound 5-chloro-*N*-phenyl-9*H*-pyrimido[4,5-*b*]indole-2,4-diamine designed by Gangjee and co-authors, as a tricyclic ATP-competitive VEGFR-2 selective inhibitor [7]. All of the docked ligands and the reference compound obtain a flat aromatic tricyclic ring system connected via a polar flexible NH linker to a hydrophobic aryl moiety as illustrated in (Fig. 3). Therefore, we have this compound as a published reference for the molecular docking and to compare its binding mode with our target compounds. It was also noticed that compound (**9d**) exhibited the most potent VEGFR-2 inhibition while compounds (**9c** and **11a**) exhibited moderate and lowest activities, respectively. The docking studies have given a partial explanation for the differential binding of these compounds to the VEGFR-2 kinase active site. The binding poses of 5-chloro-*N*-phenyl-9*H*-pyrimido[4,5-*b*]indole-2,4-diamine and compounds (**9d**, **9c** and **11a**) are shown in (Figs. 3–6).

The binding site of ATP-competitive inhibitors in VEGFR-2 kinase consists mainly of a hinge region, containing two major amino acids Cys917 and Glu915, and a hydrophobic binding site (hydrophobic region I) created by Val846, Ala864 and Val914 among others (Figs. 3–6) [7,14].

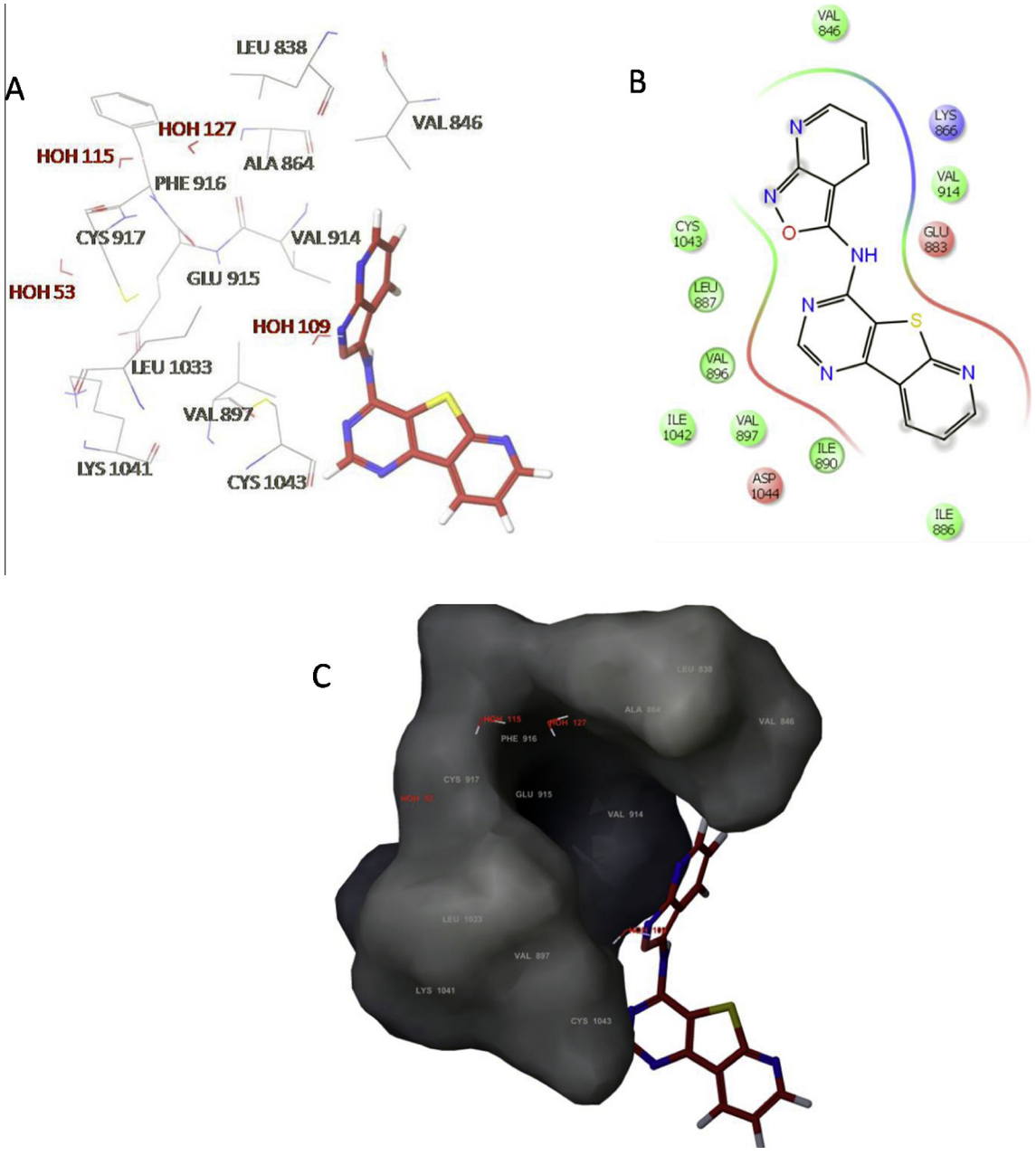

Fig. 6. Docking of compound (**11a**) in the kinase binding domain of VEGFR-2 (PDB code: 1YWN).

Docking of 5-chloro-*N*-phenyl-9*H*-pyrimido[4,5-*b*]indole-2,4-diamine resulted in a docking score of −9.12 kJ/mol with RMSD value 1.99 Å and a major hydrogen bonding interaction with Cys917 was observed in the hinge region (Fig. 3). This cysteine residue, which is unique for VEGFR-2 kinase active site, plays a crucial role in the recognition of ligands [17]. It was also noticed that this pyrimido[4,5-*b*]indole derivative which possess a relatively small aniline portion compared to the large extended hydrophobic region I. In addition, this compound did not exploit the hydrophobic pocket created by Val897, Cys1043 and Leu1033 (Fig. 3). This might explain its weak VEGFR-2 inhibitory activity.

Insight into the docked structure of compound (**9d**) showed that this compound fits plausibly in the receptor cavity. The N-3 and N–H atoms of the pyrido[3′,2′:4,5]thieno[3,2-*d*]pyrimidine core were involved in the highly conserved bidentate hydrogen bond interactions with the key VEGFR-2 residue Cys917 in the hinge region of the ATP binding site as also seen for the reference compound. The 7,9-dimethyl substituted pyrido[3′,2′:4,5]thieno[3,2-*d*]pyrimidine moiety extended towards the hydrophobic region I and was involved in the interactions with Ala864 and Val914. In the other end of the ATP-binding pocket, the hydrophobic interactions of 4,6-dimethylthieno[2,3-*b*]pyridine moiety with Val897, Cys1043 and Leu1033 are indicated to play an important role in stabilizing the three dimensional structure of the inhibitor–enzyme complex. These additional interactions, which could not be observed in the reference compound, could possibly explain the higher activity of compound (**9d**) (Fig. 4). Therefore, compound (**9d**) achieved a high docking score −7.99 kJ/mol with RMSD value 2.09 Å and a highly selective inhibitory activity against VEGFR-2 kinase with an IC_{50} value 2.6 μM.

Compound (**9c**) showed a moderate docking score −5.12 kJ/mol with RMSD value of 3.55 Å and a moderate inhibition (47%) of VEGFR-2 activity at the concentration 10 μM. The docking pose of compound (**9c**) showed that the ligand was slightly shifted outwards at the binding domain (Fig. 5). Although compound (**9c**) lacked the essential interaction with Cys917, docking indicated a favourable electrostatic interaction between the thiophene ring of thieno[2,3-*b*]pyridine moiety and Arg1030. This finding could probably suggest that the pyrido[3′,2′:4,5]thieno[3,2-*d*]pyrimidin-4-amine derivatives bearing thieno[2,3-*b*]pyridine moieties at position 4 are promising leads. These derivatives could be optimized for the development of novel VEGFR-2 inhibitors in the future investigations.

Compound (**11a**) had a low docking score +2.14 kJ/mol with RMSD value of 6.59 Å and a very weak inhibition (6%) of VEGFR-2 activity at the concentration 10 μM. The docking pose of compound (**11a**) showed that the ligand core protruded outside the receptor cavity to avoid steric clashes between isoxazolo[3,4-*b*]pyridine moiety and the polar parts of the amino acids Cys917 and Glu915 (Fig. 6).

4. Conclusion

ATP-Competitive VEGFR-2 selective inhibitors represent an important and still emerging class of safe anticancer agents that down regulates oncogenic signal pathways involved in the tumour angiogenesis and metastasis. The high degree of structural conservation amongst different kinases indicates that the development of potent and selective kinase inhibitors is a significant challenge. Inspired by the scaffolds of the previously reported ATP-competitive VEGFR-2 inhibitors, a novel series of tricyclic pyrido[3′,2′:4,5]thieno[3,2-*d*]pyrimidin-4-amine derivatives bearing bicyclic heteroaryl amines at position 4 were designed and synthesized. The rational of our study was based on the development of ATP-competitive VEGFR-2 selective inhibitors. This was probably executed by the biological studies and the molecular docking. The biological studies led to the identification of a novel inhibitor (**9d**) that selectively inhibits VEGFR-2/KDR over the six human kinases, as mentioned before, with an IC_{50} value 2.6 μM. In addition, the molecular docking of this compound showed that its core structure formed the essential hydrogen bonding interaction with Cys917 in the adenine region of the ATP binding site. The 4,6-dimethylthieno[2,3-*b*]pyridine moiety formed hydrophobic interactions with Val897, Cys1043 and Leu1033 in the other end of the ATP binding site. These hydrophobic interactions possibly play an important role in stabilizing the three dimensional structure of the inhibitor–enzyme complex. The compounds reported in this study represent a new generation of lead compounds that could help in the design of clinically useful ATP-competitive VEGFR-2 selective inhibitors.

Acknowledgments

The authors are grateful to BPS Bioscience for performing kinase inhibitory assays.

References

[1] M.I. Shahin, D.A.A.E. Ella, N.S.M. Ismail, K.A.M. Abouzid, Bioorg. Chem. 56 (2014) 16–26.
[2] K. Abouzid, S. Shouman, Bioorg. Med. Chem. 16 (2008) 7543–7551.
[3] C.J. Robinson, S.E. Stringer, J. Cell Sci. 114 (2001) 853–865.
[4] H.S. Cho, D.J. Leahy, Science 297 (2002) 1330–1333.
[5] M. Shibuya, Genes Cancer 2 (2011) 1097–1105.
[6] J. Zhang, P.L. Yang, N.S. Gray, Nat. Rev. Cancer 9 (2009) 28–39.
[7] A. Gangjee, N. Zaware, S. Raghavan, B.C. Disch, J.E. Thorpe, A. Bastian, M.A. Ihnat, Bioorg. Med. Chem. 21 (2013) 1857–1864.
[8] F. Musumeci, M. Radi, C. Brullo, S. Schenone, J. Med. Chem. 55 (2012) 10797–10822.
[9] O. Fedorov, S. Muller, S. Knapp, Nat. Chem. Biol. 6 (2010) 166–169.
[10] M.S.A. Elsayed, M.E. El-Araby, R.A.T. Serya, A.H. El-Khatib, M.W. Linscheid, K.A.M. Abouzid, Eur. J. Med. Chem. 61 (2013) 122–131.
[11] S. Shinkaruk, M. Bayle, G. Laïn, G. Déléris, Curr. Med. Chem. Anticancer Agents 3 (2003) 95–117.
[12] N. Ferrara, Oncologist 9 (2003) 2–10.
[13] A. Hoeben, B. Landuyt, M.S. Highley, H. Wildiers, A.T.V. Oosterom, E.A.D. Bruijn, Pharmacol. Rev. 56 (2004) 549–580.
[14] S. Dakshanamurthy, M. Kim, M.L. Browna, S.W. Byers, Bioorg. Med. Chem. Lett. 17 (2007) 4551–4556.
[15] L.A. Sullivan, R.A. Brekken, MAbs 2 (2010) 165–175.
[16] M.J. Munchhof, J.S. Beebe, J.M. Casavant, B.A. Cooper, J.L. Doty, R.C. Higdon, S.M. Hillerman, C.I. Soderstrom, E.A. Knauth, M.A. Marx, A.M.K. Rossi, S.B. Sobolov, J. Sun, Bioorg. Med. Chem. Lett. 14 (2004) 21–24.
[17] K. Lee, K. Jeong, Y. Lee, J.Y. Song, M.S. Kim, G.S. Lee, Y. Kim, Eur. J. Med. Chem. 45 (2010) 5420–5427.
[18] A. Gangjee, S. Kurup, M.A. Ihnat, J.E. Thorpe, S.S. Shenoy, Bioorg. Med. Chem. 18 (2010) 3575–3587.
[19] T.R. Rheault, T.R. Caferro, S.H. Dickerson, K.H. Donaldson, M.D. Gaul, A.S. Goetz, R.J. Mullin, O.B. McDonald, K.G. Petrov, D.W. Rusnak, L.M. Shewchuk, G.M. Spehar, A.T. Truesdale, D.E. Vanderwall, E.R. Woode, D.E. Uehling, Bioorg. Med. Chem. Lett. 19 (2009) 817–820.
[20] S. Pédeboscq, D. Gravier, F. Casadebaig, G. Hou, A. Gissot, C. Rey, F. Ichas, F.D. Giorgi, L. Lartigue, J. Pometan, Eur. J. Med. Chem. 45 (2010) 2473–2479.
[21] E. Perspicace, V. Jouan-Hureaux, R. Ragno, F. Ballante, S. Sartini, C.L. Motta, F.D. Settimo, B. Chen, G. Kirsch, S. Schneider, B. Faivre, S. Hesse, Eur. J. Med. Chem. 63 (2013) 765–781.
[22] S. Lü, W. Zheng, L. Ji, Q. Luo, X. Hao, X. Li, F. Wang, Eur. J. Med. Chem. 61 (2013) 84–94.
[23] R. Zheng, W. Zhang, L.T. Yu, S.Y. Yang, L. Yang, Acta. Cryst. 65 (2009) 9–16.
[24] V.I. Shvedov, T.P. Sycheva, T.V. Sakovich, Khim. Geterotsikl. Soedin. 10 (1979) 1331–1335.
[25] S.H. Jung, J.H. Ahn, S.K. Park, J.K. Choi, Bull. Kor. Chem. Soc. 23 (2002) 149–150.
[26] V.I. Shvedov, T.P. Sycheva, T.V. Sakovich, Khim. Geterotsikl. Soedin. 10 (1979) 1336–1339.
[27] Y.W. Ho, J. Chin. Chem. Soc. 48 (2001) 1163–1174.
[28] V.I. Shvedov, T.P. Sycheva, T.V. Sakovich, Khim. Geterotsikl. Soedin. 10 (1979) 1340–1342.
[29] M.R. Prasad, J. Prashanth, K. Shilpa, D.P. Kishore, Chem. Pharm. Bull. 55 (2007) 557–560.
[30] X. Florence, S. Sebille, P.D. Tullio, P. Lebrun, B. Pirotte, Bioorg. Med. Chem. 17 (2009) 7723–7731.
[31] Y.A. Kaigorodova, V.K. Vasilin, L.D. Konyushkin, Y.B. Usova, G.D. Krapivin, Molecules 5 (2000) 1085–1093.

[32] N.M. Rateba, H. Abdelaziza, H.F. Zohdia, J. Sulfur Chem. 32 (2011) 345–354.
[33] F.A. Yassin, Chem. Heterocycl. Compd. 45 (2009) 35–41.
[34] D.S. Kundariya, B.M. Bheshdadia, N.K. Joshi, P.K. Patel, Int. J. Chem. Tech. Res. 3 (2011) 238–243.
[35] K. Poreba, J. Wietrzyk, A. Opolski, Acta Pol. Pharm. 60 (2003) 293–301.
[36] http://www.bpsbioscience.com/biochemical-based-assays.
[37] A.S.A. Yassen, H.A.A. Elshihawy, M.M.A. Said, K.A.M. Abouzid, Chem. Pharm. Bull. 62 (2014) 454–466.
[38] M.W. Karaman, S. Herrgard, D.K. Treiber, P. Gallant, C.E. Atteridge, B.T. Campbell, K.W. Chan, P. Ciceri, M.I. Davis, P.T. Edeen, R. Faraoni, M. Floyd, J.P. Hunt, D.J. Lockhart, Z.V. Milanov, M.J. Morrison, G. Pallares, H.K. Patel, S. Pritchard, L.M. Wodicka, P.P. Zarrinkar, Nat. Biotechnol. 26 (2008) 127–132.
[39] This Work is submitted to Academy of Scientific Research and Technology, Egyptian Patent Office, Number 1468/2014.
[40] Y. Miyazaki, M. Nakano, H. Sato, A.T. Truesdale, J.D. Stuart, E.N. Nartey, K.E. Hightower, L. Kane-Carson, Bioorg. Med. Chem. Lett. 17 (2007) 250–254.